

Experimental setup for CO₂ injection for Enhance Shale Gas Recovery (ESGR) - A Review

Ashwani Kumar , Nivedhan D. N , Tiburtius Rajesther S.
University of Petroleum and Energy Studies

Abstract:- Approach of Carbon capture and sequestration (CCS) and injection in shale formation in order to maximize methane recovery by CO₂ adsorption and simultaneously storing anthropogenic gas in subsurface making the whole process as carbon-neutral (subjecting carbon from where it has originally come from). Environmental degradation and energy crises could be stopped by developing innovative shale gas production methods. This article reviews published literature on an experimental setup for shale gas recovery by the adsorption/desorption mechanism of carbon dioxide and methane gas on shale rock. Complete knowledge of carbon-dioxide sorption mechanism and characterization on shale rock with technical aspects discussed in this article. Data stated by published information on an experimental setup reviewed on the basis of different adsorption isotherms on distinct shale samples from all over the globe. Geological specifications such as TOC, porosity/permeability, moisture content, shrinkage/swelling and flow behavior as crucial conditions for CH₄, CO₂, and N₂ gas adsorption in shale discussed. Effects of injecting gases on petrophysical properties of shale rock. Supercritical CO₂ influence on natural gas recovery from shale gas reservoir and methodology.

1. INTRODUCTION

Anthropogenic carbon dioxide release in the environment due to burning fossil fuel which has resulted in global warming that's why environmentalists are facing major issues about increasing atmospheric temperature and pollution level. Recent advancement in better fracturing techniques and multi-layer horizontal drilling methods results in bringing unconventional shale gas energy into the mainstream. Shale gas development has proven to be a game changer for the United States of America greatly impacting natural gas economics, carbon saturation in the environment, and energy independence with reserves projected to last for around 100 years, as well as energy security across the globe[1]. According to the Energy Information Administration(EIA) shale gas holds a large proportion of unconventional energy sources in the earth as the estimation of technically producible shale gas is 6,622 TCF(Trillion Cubic Feet). If the method includes CO₂ injection for production then it can result in storing around 26,114GT of CO₂ in subsurface as used for pressure maintenance or for producing natural gas as Enhance Shale Gas Recovery(ESGR) method. Countries like the US, Canada, Algeria, Argentina, and China have already converted shale producing natural gas economically viable by mass production.

Shale formation acts as the source rock as well as reservoir rock and termed as shale plays or shale gas unconventional reservoirs. Hydrocarbons cooked in shale but do not migrate. Maturity of shale mainly depends on the depositional environment, clay content, formation temperature, kerogen type and TOC percentage. Shales rock are elongated layers for several kilometers with very low permeability but good hydrocarbon holding capacity. Horizontally, drilled wells through elongated formations give maximum exposure to stored natural gas in the fine pores of shale matrix.

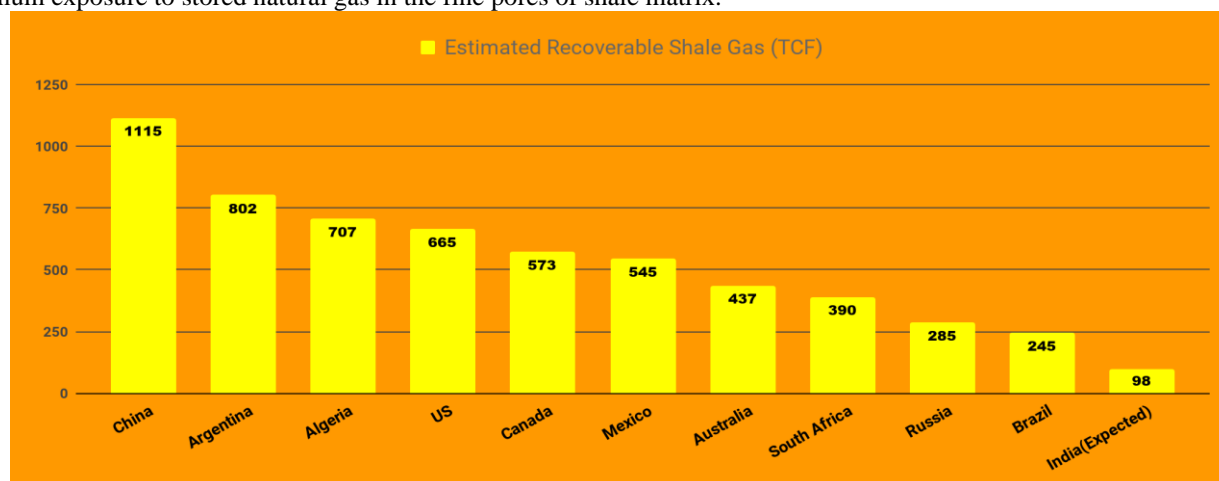


Fig.1 Countries with recoverable shale gas reserves

In recent years, CO₂ injection in shale formations has been investigated with the aim to enhance shale gas recovery (ESGR) and permanently storing CO₂ gas in shale matrix which is accounted to 95-99% of the total gas fraction injected[2]. Injecting mixtures of CO₂ and N₂ may potentially optimize recovery of natural gas and beneficially sequester CO₂. Several studies specify that CO₂ adsorption rate on shale is five times higher than that of CH₄. The ESGR method is embryonic as pre-adsorbed methane gas gets released by the influence of CO₂ because of the resulting in-situ swapping mechanism at the sorption site. The shale formation consists of different pore sizes, pore distribution, and interconnectivity and plays a major role in

understanding competitive analysis and gas flow dynamics in shale. Models of experimental setup are developed to analyze the gas flow dynamics by assuming formation as homogeneous. But it is not possible to model the fluid flow in stimulated fractures[4].

This paper review published information on experimental data explaining enhanced methane recovery with injection of carbon dioxide and nitrogen gases. Experimental model shows the impact of displacing fluids CO₂ and N₂ on CH₄ recovery and gas flow dynamics in shale matrix. Coats–Smith dispersion– capacitance models(Coats & Smith, 1964) explaining dispersion in porous media gives short breakthrough time for N₂ and lesser recovery rate and longest breakthrough time for CO₂ and higher rate of recovery. Give a brief idea of shrinkage effect because of N₂ increasing permeability and swelling because of CO₂ injection closing fracture decreasing permeability. Low field Nuclear Magnetic Resonance Technique (LF NMR) is used to determine that apart from the affinity of CO₂ to get adsorb at shale surface what other changes take place[5]. To understand the flow of CO₂ in the shale matrix instrument is provided with a pressure pulse transmission test. Calculating of gas permeability, viscosity flow mechanics, adsorption affinity of CO₂/N₂ calculated in this paper. Apparent permeability estimation model along with Pulse decay experiment is used to calculate porosity in the adsorbed phase after the interaction of CO₂ with shale. Allover estimating gas flow capacity through shale by Langmuir heterogeneous adsorption isotherm, Simplified local-density (SLD) to calculate CO₂ adsorption on shale, Equation of State (EOS)[6], Elliott-Suresh-Donohue (ESD)[6], Brunauer–Emmett–Teller (BET) isotherm[7], Gibbs Free Adsorption process equations, LF NMR(low-field nuclear magnetic resonance) and operating systems is used to calculate adsorption rate and process on the different type of shale.

2. APPARATUS

Gas injection in shale samples along with observation of adsorption/desorption rate is a typical process as it depends on material property. On the basis of various published literature on experimental models for CO₂ injection on shale samples, we have come up with the most basic and simple model consisting of all required equipment for measurement of shale properties.

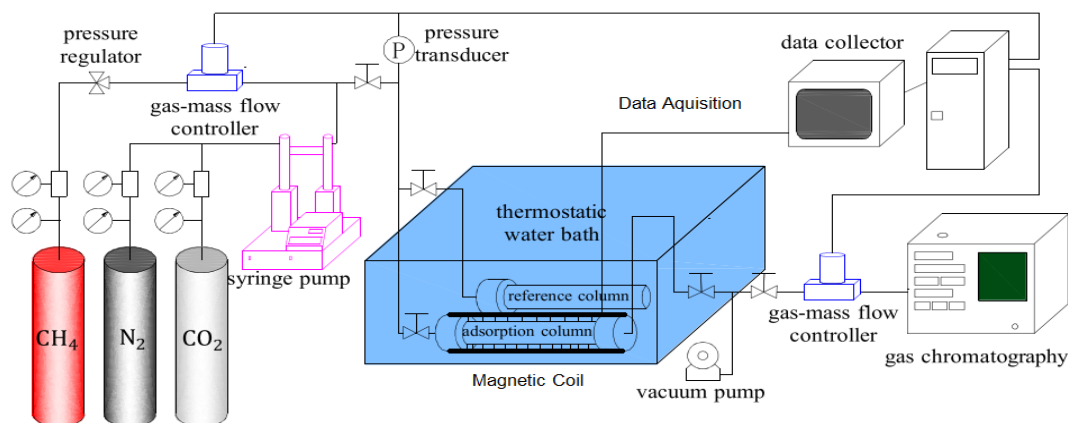


Fig. 2 Schematic experimental model to estimate changes in shale samples after subjecting it to different gases. (Huang, Xue & Li, 2020)

Highly pressurized gas cylinders(CO₂,N₂,CH₄) attached to the infusion syringe pump. These pumps play a major role and are a crucial component in production and estimation of gas samples from shale when using supercritical fluids such as carbon dioxide. Syringe pump function is to increase and control gas pressure for injection("KSB to equip Libyan pumping stations", 2006). Thermostatic water bath system with fluctuation range less than ± 0.1 °C was introduced to the experiment to maintain temperature in the reference cell and adsorption column. Gas chromatograph used to calculate the composition of gas coming out of the adsorption column of the gas-mass flow controller to measure and control gas flow. Data collector, computer setup installed with relative software such as LF NMR(Huang, Xue & Li, 2020).

3. MATERIALS AND CHARACTERISATION

Core samples from different basins are studied by various experimental setups by different authors all around the globe. Shale rock is mainly characterized on the basis of clay material and Total Organic Content(TOC).

Basin	Location	TOC %	Clay Content %	Sample Depth(m)	Literature
Perth Basin	Western Australia	0.23-3.03	28-56		(Zou et al., 2018)
Gulf Basin	Gulf of Mexico	0.11-1.30	38-54	2900-3300	(Mahmoud et al., 2020)
Ordos Basin	China	0.21-2.43	32-56	2250-2400	(Liu, Agarwal & Li, 2020)
Sichuan Basin	China	0.75-2.5	64-79	2800-3000	

Fig.3 Samples studies in review paper from different basins in world

Maturity characterisation of shale rock samples were done using the same basic methods in every experiment. Rock eval for TOC, type and thermal maturity level of organic content monitored using Flame ionization detector. Shale samples heated at temperature 340-650 degree celsius to estimate hydrocarbon quantity in the sample.

The X-ray diffraction method(Fig.4) is used to calculate the material composition of different shale samples in most of the published literature because of the method's efficiency. X-Ray Diffraction peaks generated by effective interference of a monochromatic collection of X-rays dissipated at specific angles from each set of lattice planes in a sample. Fig.4 Scanning electron microscopy(SEM) is a microscope which produces an image of the surface of a sample inducted to a concentrated beam of electrons. Method clearly gives information about the surface composition of the material sample in our case shale.

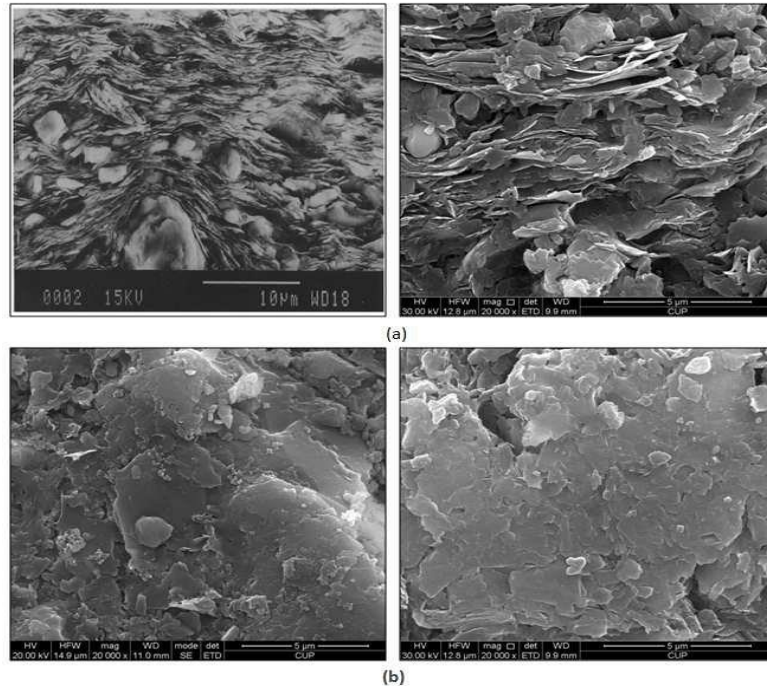


Fig.4 SEM image of shale sample clearly shows complex instructure geometries, high density, lower porosity and permeability.

Fourier transform infrared spectroscopy method is used to identify the deposition environment of sedimentary basins for different source rocks. This method shows the fine difference of the organic matter and organic carbon such as kerogen types, total organic content and hydrocarbon structure in rock.

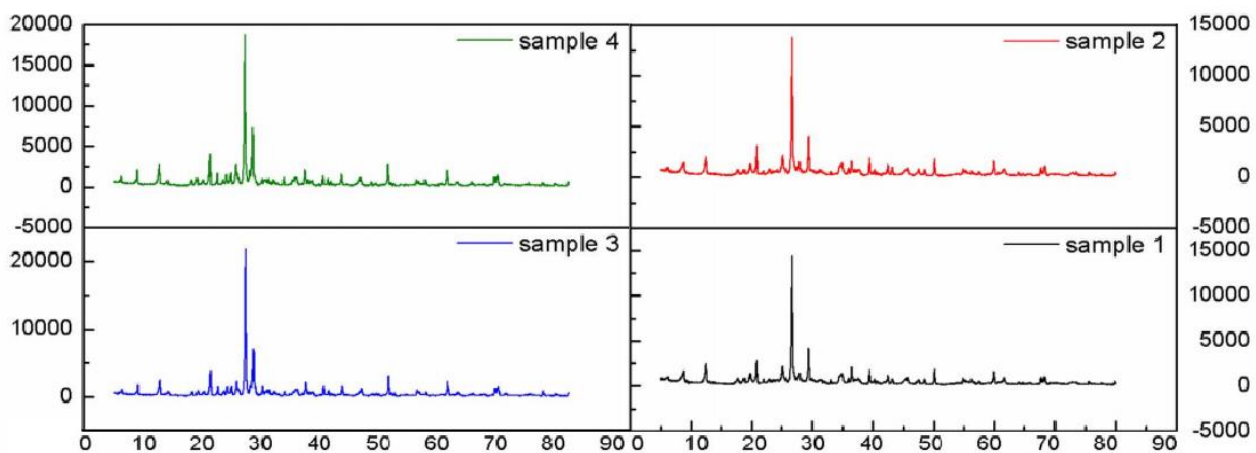


Fig.5 X-Ray diffraction patterns of shalesDegree - 20 Two peaks at 25° and 45° show similar peaks in all samples. Samples having lower organic content will show high peaks comparatively(Huo et al., 2020).

4. EXPERIMENTAL PROCEDURE

While going through different published literature on experimental setups to measure the adsorption rate of CO₂/N₂ gas on shale, everywhere one basic method is adopted as compiled below. The shale rock samples with a total organic composition ranging 0.11-3.03% studied from different locations all over the globe. The sample is crushed and sized into 0.0075-0.085 cm fragments while some were used as a solid core in the experiment. Samples are then heated in the oven at 383K for 24hr at most to remove moisture and impurities. The measured amount of treated sample is subjected in a sample chamber and vacuumed for 5hr straight.

Helium gas used for leak testing at 10MPa and to calculate the void volume by helium expansion at 1-7 MPa and the final value used was average of different pressures.

Adsorption column in experimental setup is treated with methane at different pressures ranging from 5-15MPa at 318K and left for 4-10 hours for adsorption until pressure reaches the equilibrium stage. After reaching equilibrium pressure stage displacing fluid such as carbon dioxide and nitrogen gas injected to an adsorption column in different proportions such as 100% of CO₂, 100% of N₂, 50-50% ratio of CO₂/N₂ mixture, 20-80% ratio of CO₂/N₂, and 80-20% ratio of CO₂/N₂ mixture. The outlet valve in the model opened simultaneously to collect released methane gas from the rock sample. Flow rate for injection kept at 10 milliliters per minute and adsorption column at 10 MPa. The CO₂/N₂ injected in the adsorption chamber as liquid to displace the methane gas by its greater affinity towards shale rock. Hence, methane gas as a free gas desorb from shale surface and comes out of the outlet valve. Gases composition coming out of adsorption chambers in the experimental model collected in a mass flow collector and composition percentage calculated by gas chromatograph. Experiments stop when the mole fraction of methane reduces to 2% in the samples.

5. ADSORPTION/DESORPTION MECHANISM

In shale gas, a large proportion of natural gases(CH₄, C₂H₆) are found in the adsorbed state, while some proportions are in free state depending on kerogen type, TOC content and maturity of shale. Shale has 10-30 times less gas adsorption capacity than coal for its lesser content of organic matter. The clay minerals in shale can hold up to 10% of adsorbed gas and methane adsorption capacity of shale have the clay minerals arranged in the order of Montmorillonite > Illite/Smectite mixed layer > Kaolinite> Chlorite> Illite(Rani, Padmanabhan, & Prusty, 2019).

Fluid interaction with shale results in change in porosity and permeability that greatly depends on physical and chemical properties of rock and influencing fluid. A higher capillary pressure impedes the flow of CO₂ through shale(Bhuiyan, Agofack, Gawel, & Cerasi, 2020). Nearly 40-50 % of total gas stored in shale formation by adsorption mechanism. Adsorption isotherm mainly uses gravimetric, volumetric and chromatographic techniques to estimate adsorption volume such as the Langmuir model, BET (Brunauer-Emmett-Teller) model and Dubinin-Polanyi model. Mechanism of physisorption is responsible for adsorption and gas storage in shale and weak Van Der Waals forces are responsible for holding gas molecules in the shale matrix. The highly fractured brittle shale rock formations known to be best suited for CO₂ sequestration of gas flooding and with increasing permeability of formation, the CO₂ sequestration will also increase. Adsorption is a surface phenomenon where pore volume gets filled by influence of the subject gases in our case CO₂, CH₄ and N₂. Adsorption of gases on shale is greatly influenced by type of adsorbent, pressure/temperature of adsorbent and type of shale experimental analysis states that adsorption and desorption curves do not coincide with each other(Guo, Hu, Zhang, Yu, & Wang, 2017). Different Langmuir(1918) equations for both processes justified the statement. Higher the value of organic content in shale higher will be the desorption rate with the increasing pressure difference. The adsorption capacity of shale varies for different adsorbing gases. The gases injected into shale are not fully released during production. When the pressure increases, the adsorbing capacity of gases is gradually increased and has the highest adsorbing capacity in the order of CO₂, CH₄ and N₂.

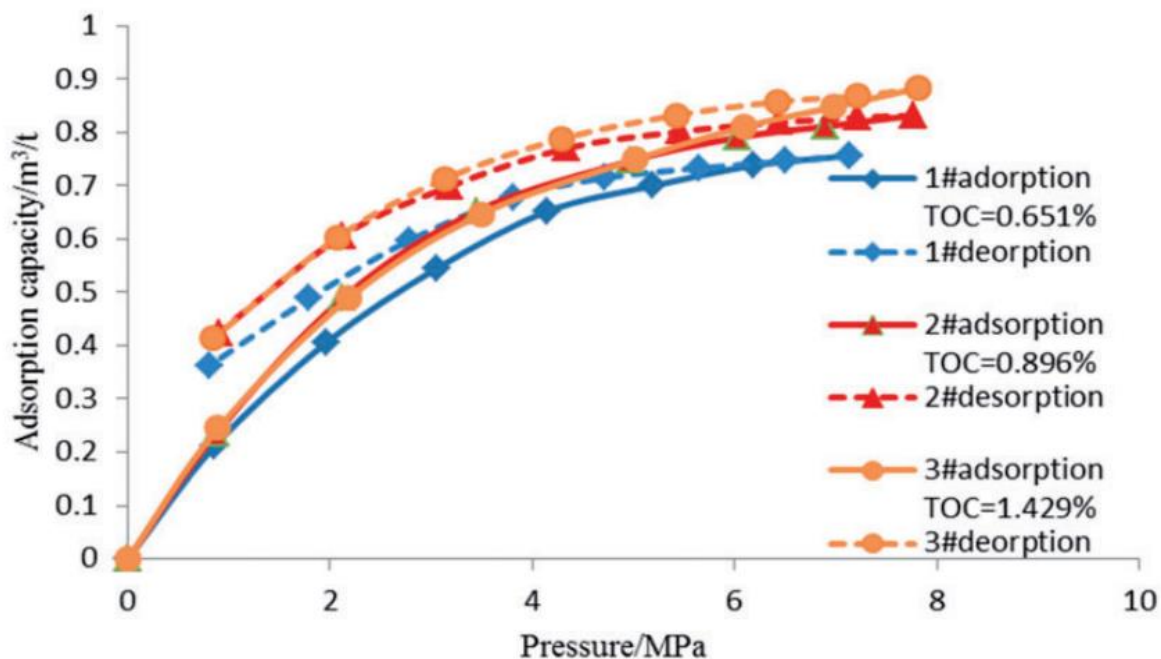


Fig.6 Adsorption and desorption curve for shale with different organic content(Guo, Hu, Zhang, Yu, & Wang, 2017)

Fig. shows shale gas adsorption at the atomic level explained using the quantum mechanics approach and adopting multi-body Schrodinger Equation. Basically, DFT was used to understand methane interaction with graphene as physically adsorbed. Methane on graphene was attached as carbon to carbon with weak van der Waals forces.

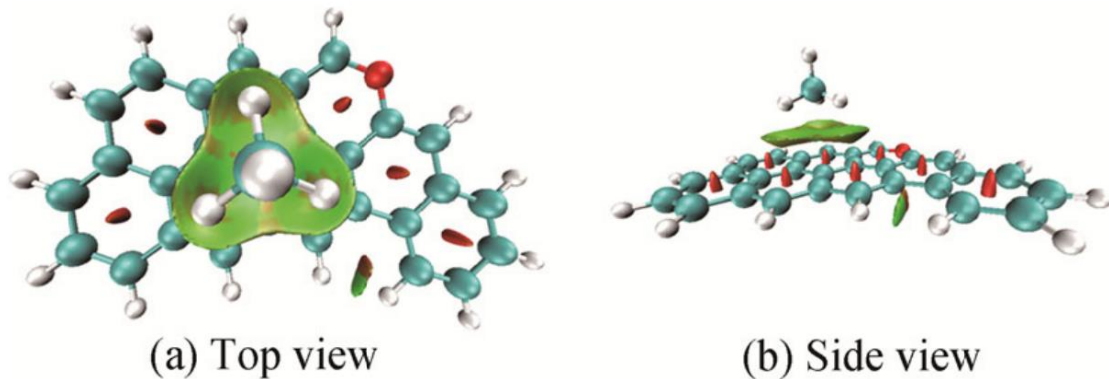


Fig.7 Graphene molecular structure treated as kerogen given as adsorption site for CH₄ attached through weak van der Waals forces(Wang, Qu, Yin, Bai, & Yu, 2018).

6. ADSORPTION CAPACITY OF CO₂/N₂

Increasing shale gas recovery by injection of CO₂, N₂ and mixture of two. The adsorbing capacity of shale varies for different adsorbing gases. The gases injected into shale are not fully released during production. When the pressure increases, the adsorbing capacity of gases gradually increases and has the highest adsorbing capacity in the order of CO₂, CH₄ and N₂(Chen, Feng, & Pan, 2018). Experimental model shows the impact of displacing fluids CO₂ and N₂ on CH₄ recovery and gas flow dynamics in shale matrix. Breakthrough curve shows the displacement of CH₄ in absorbent cells from 100% mole fraction to 4% mole fraction with injection of CO₂(Fig. 6 (a)). Two simultaneous experiments showing the exact same path of gas displacement determine reliability of data outcome. CO₂ storage capacity depends on CO₂ sorption isotherm and estimates of the ultimate recovery of gas from shale. The storage of CO₂ in the shale will affect the mineral composition, reservoir temperature and pressure.

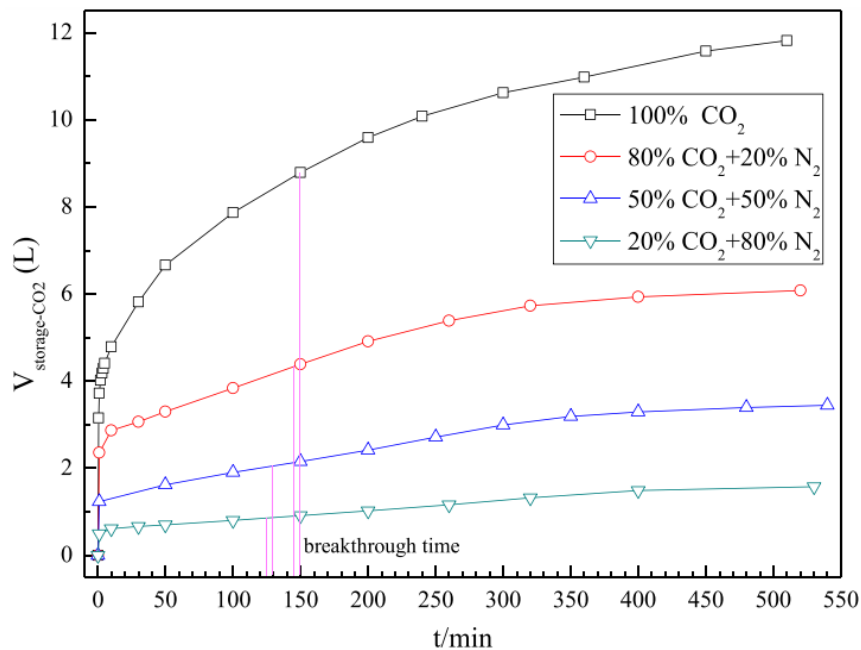


Fig.8 Adsorption of different gases on shale calculate by langmuir isotherm(Chen, Feng, & Pan, 2018)

The quantity of CO₂ adsorption is proportionate to CO₂ adsorption isotherm. Storage capacity of CO₂ calculated using Langmuir adsorption equation generally. Hike in the 20% recovery rate observed by the experimental model when using pure CO₂. Observation studies state that in two gases mixture injection CO₂ and N₂, if carbon dioxide percentage is much higher than N₂ then decreasing trend in recovery of methane is the outcome. If saturation of CO₂ is greater in mixture by 70% then sequestration and storage rate of anthropogenic gas is quite low in subsurface shale formation. This is because, higher proportion of CO₂ indicates lesser recovery, which states that limited sites will get free where methane was previously adsorbed. These sites in the shale matrix are places where CO₂ will be getting absorbed. Injecting mixture of both gases (CO₂ and N₂) gives better results in pressure maintenance. N₂ gas adsorption affinity towards shale rock is quite lower than CO₂, and N₂ moves in perfect

piston-like movement in low permeable highly confined regions pushing CH₄ in very small capillaries towards hydrocarbon producing zones. Researchers' experiments in published literature follows Langmuir isotherm for homogeneous shale formation. General estimation states that adsorption affinity of N₂, CH₄, and CO₂ gas on shale in the ratio of 2:3:5. The whole process in shale ESGR deals with adsorption and desorption of CH₄, CO₂ and N₂ gas. In nutshell methane ejects from adsorption because of higher affinity of carbon dioxide gas towards clay surface and nitrogen gas flowing in rock matrix at relatively higher pressure pushes desorb methane gas increasing permeability of formation (Li & Elsworth, 2019).

Fig. 8 This graph is defining storage capacity of CO₂ for all four kinds of injection cases. Shows that maximum storage is for single component gas injection with greatest breakthrough time and as the concentration of CO₂ decreases in gas injection storage and breakthrough time also decreases.

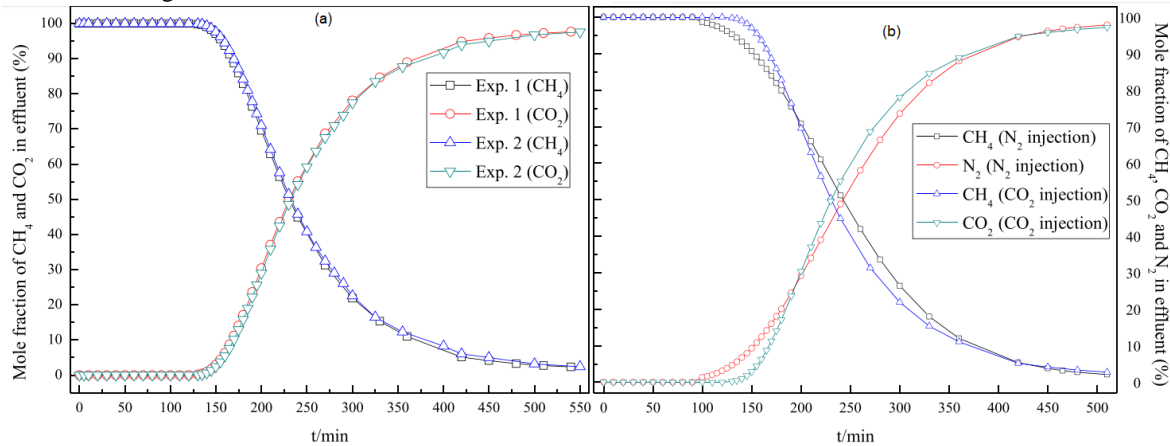


Fig.8 Mole fraction CH₄, CO₂ and N₂

This graph(Fig.8) shows the flow of displacing fluid in two assumed sections of shale reservoir rock stagnant and flowing region. N₂ mainly deals with the easy flowing region in free state and acts as displacing agent by sweeping CH₄ from meso and macro fractures to microfractures. CO₂ deals with the restricted zone of formation as it flows into micropores because of linear molecular shape. This also shows that migrations of injected CO₂ and N₂ along the adsorption column are different. This graph indicates the dependency of experiment displacing methane by injection of carbon dioxide. Breakthrough curve shows displacement of CH₄ in absorbent cell from 100% mole fraction to 4% mole fraction with injection of CO₂. Two simultaneous experiments showing the exact same path of gas displacement determine reliability of data outcome.

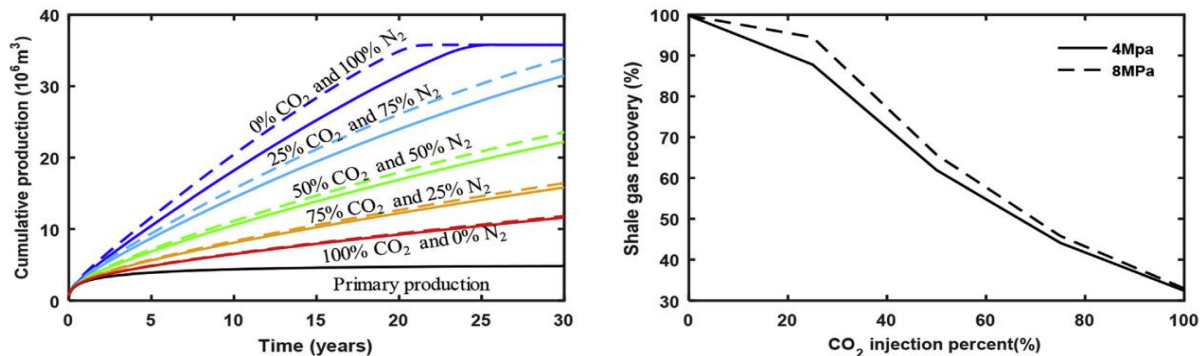


Fig. 9 Methane production with respect to time consumed for cumulative mixture of nitrogen and carbon dioxide gases injected in different ratios at constant pressure(Li & Elsworth, 2019).

When the temperature of shale matrix increases, the adsorption of gases will decrease. So, swelling of the matrix also reduces. When the pressure in the shale increases, the adsorption of gases in the matrix increases to cause deformation even as the temperature rises. There is a sudden increase in volumetric strain due to pressure increase, and it acquires a plateau at higher pressure.

7. MOISTURE EFFECT

Moisture is a crucial subsurface component which should be analyzed in experimental procedures. The presence of moisture will lower the gas adsorption capacity of shales due to the competitiveness between methane and water molecules. The moisture content in shale will block the pore throat for the movement of methane molecules(Zhou, Jin, & Luo, 2019). It is observed that by increasing moisture content the sorption capability decreases until a certain critical moisture content percentage is achieved for the sample. The critical(equilibrium) moisture content is the highest moisture saturation that absorbs on shale matrix.

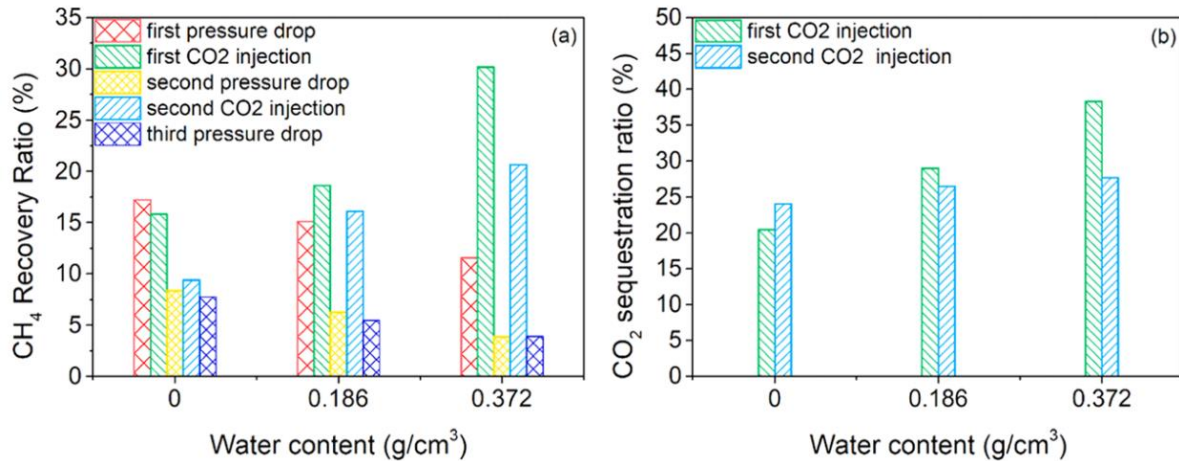


Fig.10 (a) Methane recovery and (b) Carbon dioxide adsorption on clay ratio with respect to changing water content during the shale gas recovery process in 2 nm kerogen slit pores at 338.15 K.

This bar diagram in Fig. 10(a) depicts CH₄ recovery ratio under water content ranging 0-0.372gm/cc. Observations made using bar diagram can state with rising water saturation in rock, there is a slight drawdown in first pressure drop. Therefore, in moist conditions efficiency of CO₂ injection is higher for recovery. Bar diagram (b) shows that when the moisture content of shale increases, the CO₂ sequestration ratio also increases (Fig.10). Simplified local-density (SLD) to calculate CO₂ adsorption on shale along with X-ray Diffraction (XRD) for composition calculation.

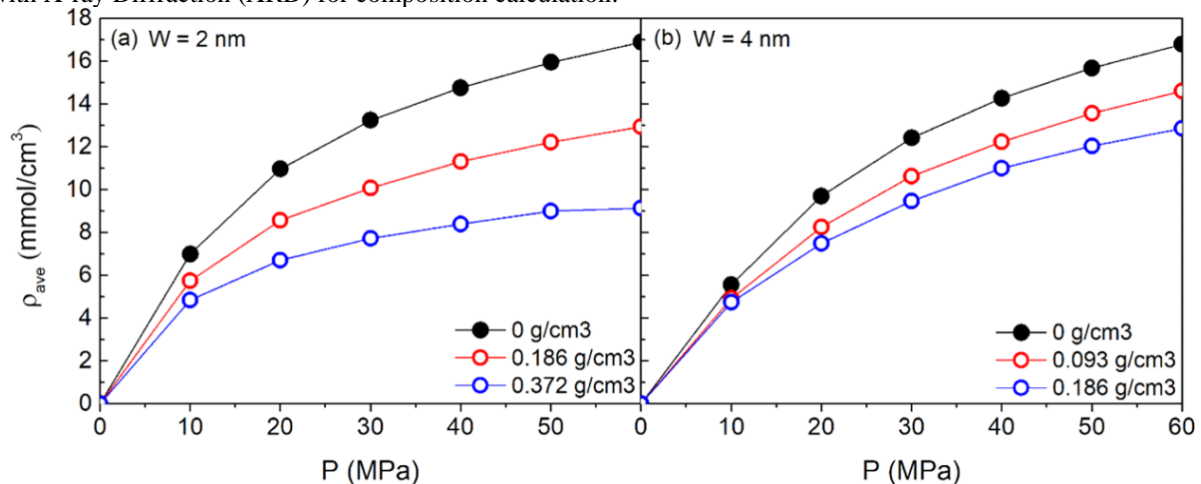


Fig.11 For pore width of (a) 2 nm and (b) 4 nm average density methane for dry and moist shale sample influence by range of temperatures.

The average density of methane gas increases with pressure increase at dry conditions and moist conditions (Fig.11). The density of CH₄ reduces in the middle of a kerogen slit pore due to the drop in pressure. After CO₂ injection, the density of CH₄ decreases near the surface of kerogen in shale gas recovery. The average density of CH₄/CO₂ mixture in kerogen increases with the pressure increase gradually and attains constant average density at certain higher pressure. As the moisture content in shale increases, it affects the performance of pressure drop. Due to the lower solubility of CH₄ in water than that of CO₂, CH₄ sorption decreases in the moist condition in the presence of CO₂.

8. EFFECT OF CO₂ ADSORPTION ON PETROPHYSICAL AND MECHANICAL PROPERTIES OF SHALE

When CO₂ is subjected to shale its porosity, and connective porosity gets increased. There will be little change in the pore structure of shale by dissolution and adsorption induced expansion. There will be a swelling of shale with an increase and then decrease in stress conditions and increase in sealing capacity. The specific surface area of shale will reduce when supercritical CO₂ dissolves in shale. When CO₂ reacts with shale, it alters mechanical properties of shale such as stiffness, strength, fracture threshold, Poisson's ratio and brittleness index.

During experimentation, the compressibility of pore fluid and the dynamic stiffness of the porous material is affected by the presence of CO₂. While the exposure of shale to CO₂, Young's modulus of shale increased by around 2% and Poisson's ratio remained constant. The swelling of shale depends mainly on clay content and water saturation. The swelling because of resulting adsorption can change the mechanical properties of shale. Brittleness Index is the ratio of reversible strain to total strain. Shale swelling will lead to alterations of brittleness index depending on the exposure of CO₂ or CO₂-H₂O.

8.1 Porosity and Permeability

The storage and swelling are the major effects considered in shale adsorption, which further results in change in permeability of shale. Permeability changes generally calculated by diffusing gas in the sample chamber and pressure pulse transmission test. Boyle's Law shows contribution to calculate detectable porosity and permeability using numerical methods. The core sample was inserted into a sample cell for the application of confined pressure. Then, the volume calibration tests are undergone to get reference chamber volume and void volume. The system was vacuumed and then supplied with methane gas with equilibrium temperature and pressure. The pressure response with time was measured while opening the valve to release the methane. Swelling in rock calculated using deformation measuring gauges all over the sample. Repetition of this process at various pressure points for accuracy of measured changes, and adsorption is calculated using volumetric method. Knudsen equation for modelling permeability of shale gas. The permeability growth rate increases for lower value of volume ratio, and it decreases gradually with increase in volume ratio (Fig. 12).

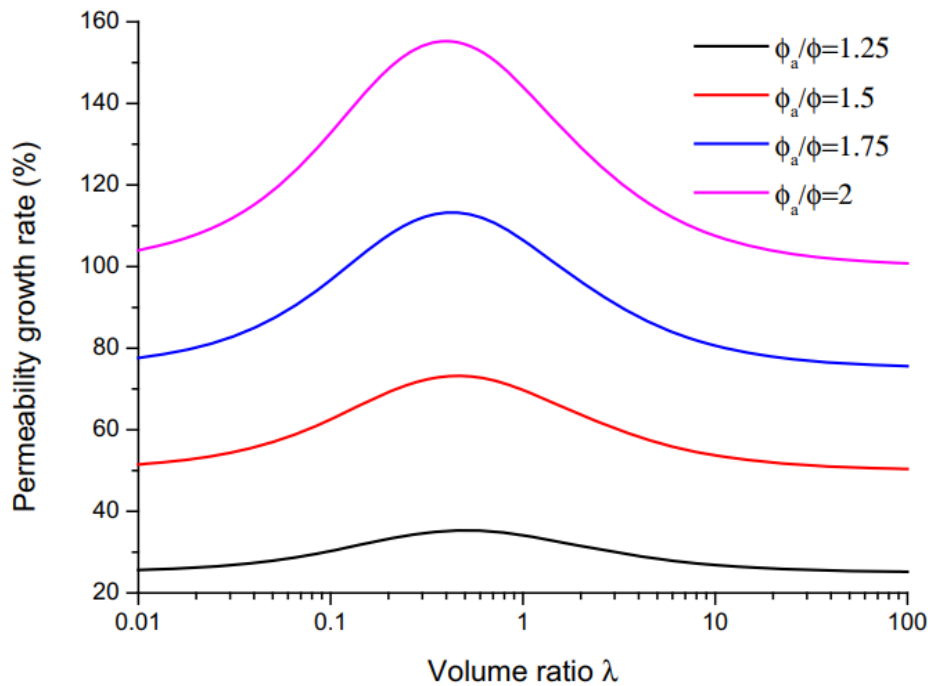


Fig.12 Permeability growth rate versus volume ratio for different ratios of apparent porosity to true porosity (Zhao, Wang, Zhang, & Liu, 2019).

Intrinsic Permeability is rock property independent of flowing condition. The ratio of intrinsic to apparent is greater than one in shale but in conventional reservoir case it is equal to unity means there is no such difference in the two permeability in sandstone reservoir. These three graphs show the relation of permeability with pressure, as trends decrease with increasing pressure. Graph's trend becomes negative when the gas phase changes to a critical point uniquely for CO₂ in this study. Permeability depends on changing the density value of gases as the difference between adsorbed density of gas to free gas density. When the gas pressure increases, the porosity of the shale matrix will increase gradually by carbon dioxide, methane, ethane, and propane. But for butane gas, the porosity alters within the initial pressure of about 20 atm.

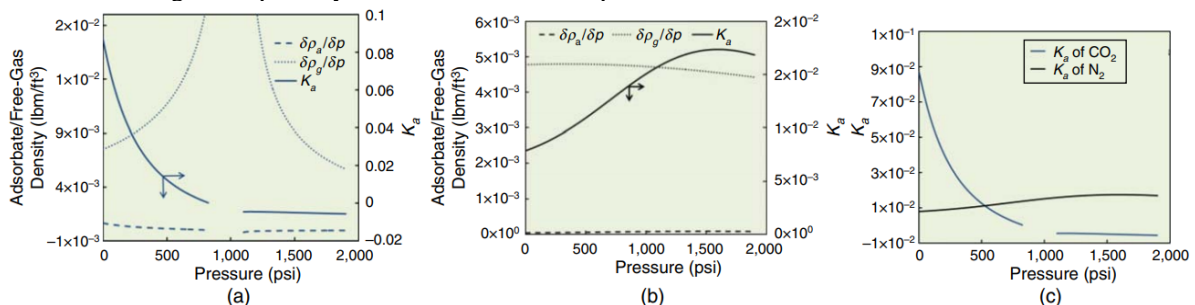


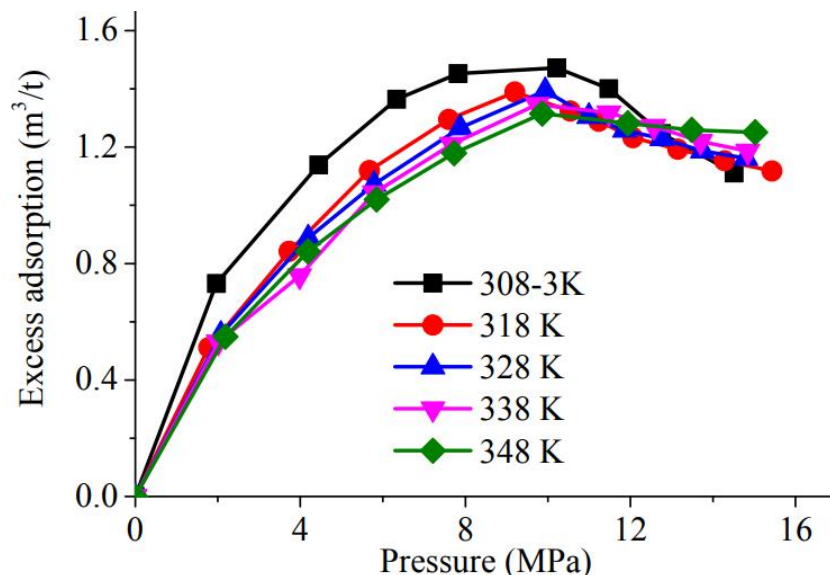
Fig.13 Graph shows a partial derivative of free gas density to differential pressure for (a) CO₂, and (b) N₂. (c) K Ratio of gibbs density to absolute density of CO₂ and N₂ (Jia, Tsau, & Barati, 2018)

8.2 Swelling/Shrinkage

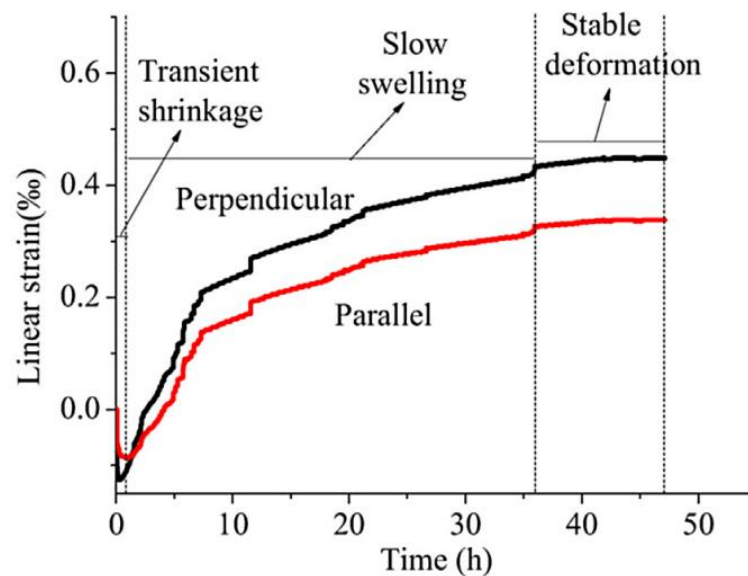
Shale swelling is an important prospect to understand CO₂ injection for methane gas recovery. Gas sorption capacity affects gas storage, matrix swelling and gas flow mechanisms in nanoporous organic rich shale gas reservoirs (Pang, Chen, Soliman, Morse, & Hu, 2019). In published literature, three kinds of shrinkage available such as transient shrinkage, slow swelling, and stable strain. Swelling occurs when CO₂ gets adsorbed on the surface of shale and tends to increase the size of pore reducing surface potential energy of shale. This response will result in a closing of fracs and reduction in permeability of formation. The

shale matrix will swell high due to the presence of gases in the sequential order of carbon dioxide, methane, ethane, and propane (Tesson & Firoozabadi, 2019). The bulk swelling and pore shrinkage of shale results from methane sorption. It was observed that sorption induced bulk swelling, which is linearly proportional to absolute gas sorption amount. Simplified local-density (SLD) to calculate CO₂ adsorption on shale, Polanyi (Polanyi, 1963) model and Duong, 1998 for better understanding of shale swelling (Lu et al., 2016). Molecular Dynamics-Grand Canonical Monte Carlo simulation, and poromechanical model they can be used to calculate deformation and swelling induce in shale because of gas adsorption.

The adsorption induced swelling strain in shale will increase sharply at initial pressure and then increases gradually with increase in pressure. Surface area, pore size distribution and porosity get reduced in the influence of CO₂. The intermolecular repulsion forces between sorbate-sorbate and sorbate-sorbent molecules will induce pressure increase in the pores, which cause increase in adsorption induced swelling strain rapidly at initial stage.



(a) Amount of excess adsorption in shale samples at different temperature



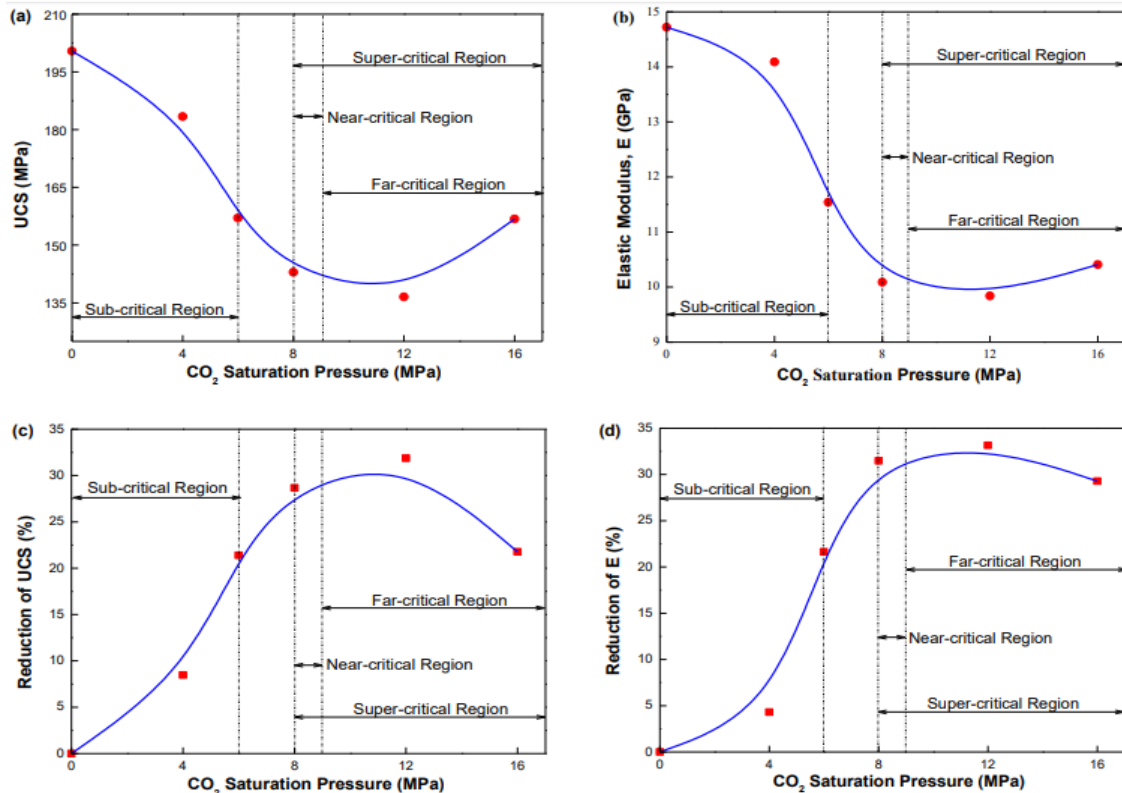
(b) Linear swelling of shale at 5MPa

Fig.14 Shrinkage on basis of adsorption rate(Chen, Feng, & Pan, 2018)

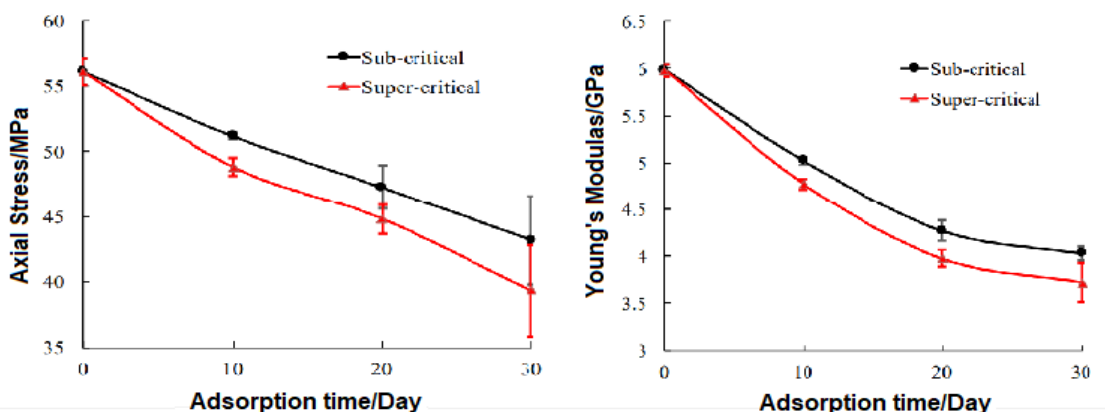
This curve (Fig. 14 (a)) shows ScAdsorption of CO₂ on shale as temperature for experiment remains above the critical temperature of carbon dioxide. This curve indicates that adsorption increases with increasing CO₂ pressure below critical pressure. After maximum pressure of range 6-9 MPa adsorption rate decreases with increasing temperature. Temperature change also attributes shale swelling or adsorption rate, as the temperature increases swelling rate decreases with decreasing volumetric strain.

Strain values used to understand swelling in shale. The swelling in shale matrix is due to strain caused by poroelasticity and gas adsorption. Graph (Fig. 14(b)) represents a change in strain in core samples with increasing time and CO₂ pressure. In transient shrinkage CO₂ gets adsorbed on sample cells increasing pore pressure and stress induces gradually. In a slow swelling

region as a lesser number of pores remain for CO₂ to get adsorb, so the rate becomes slow, and CO₂ gets absorbed in pores of greater or equivalent size. At stable strain condition adsorption reaches an equilibrium state and the effect of the effective stress and the absorption of the stress comes to a minimum. The swelling strain of adsorbing gases in shale will increase gradually with hike in gas pressure. When the mass fraction of shale increases, the strain fraction of shale due to gas pressure increases. Thus, the swelling rate of shale is directly proportional to the gas adsorption rate (Chen, Feng, & Pan, 2018). Figure (Fig. 14(a)) shows the interaction of shale with different saturation pressure of CO₂ and resulting UCS and Elastic modulus changes. One can interpret through graphs that UCS strength and Young's modulus both decrease with increasing saturation pressure of CO₂ resulting in reduction in mechanical stability of shale. Through this, one can also interpret microstructure alteration with the influence of CO₂. Resulting in the swelling of shale, adsorption/desorption, and micro cracks. A supportive graph (Fig. (b)) for previous results showing reduction in axial strength and young modulus. This degree of reduction is influenced by geo-environment characteristics of shale formations, CO₂ phase, adsorption pressure, interaction time etc. This study is also important to understand the borehole stability.



(a) Effect of CO₂ adsorption pressure and phase change on UCS and Young's modulus of shale



(b) Effect of CO₂ adsorption time on UCS and Young's modulus of shale

Fig.15 Shows changes in stress and strain conditions of shale under CO₂ adsorption (a) (Yin et al., 2017, (b) (Lyu et al., 2018b)

9. SUPERCRITICAL CO₂ ADSORPTION

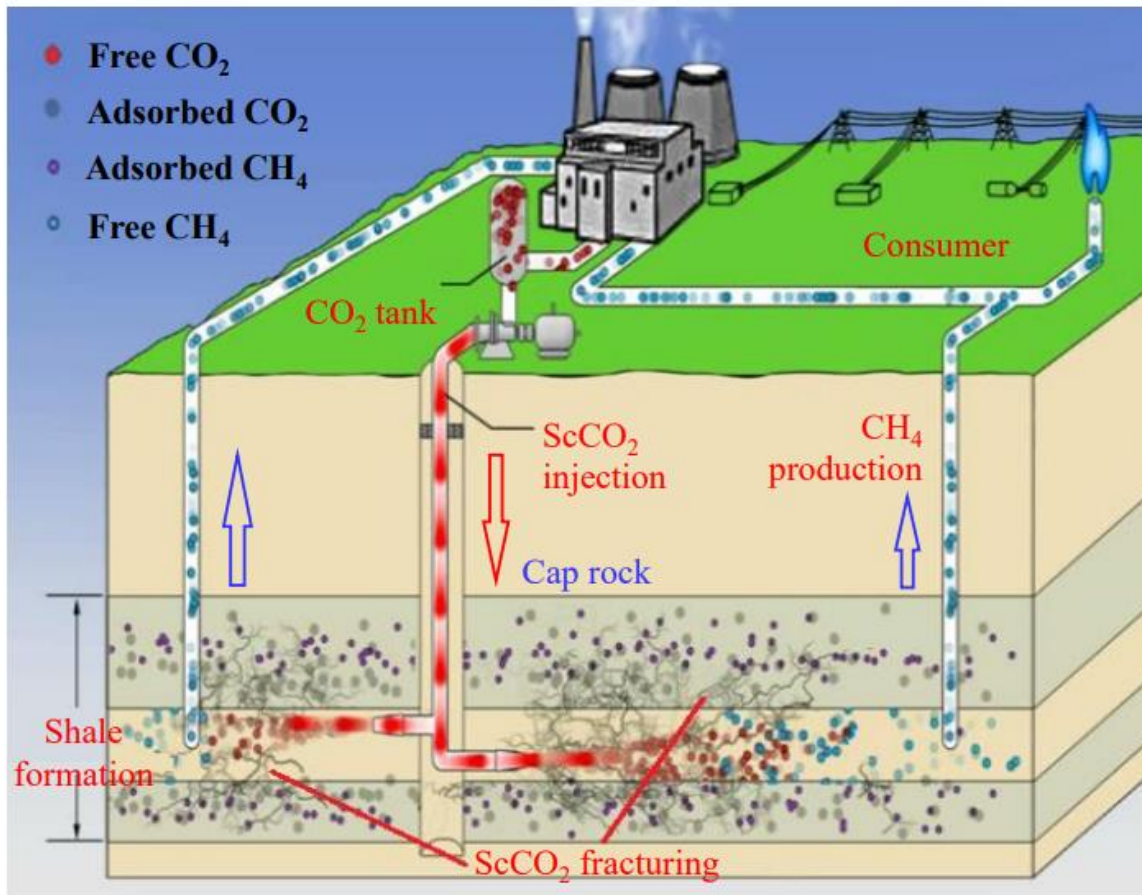


Fig.16 The schematic diagram of supercritical CO₂ fracturing for enhanced shale gas recovery and CO₂ sequestration (developed after Li and Kang, 2018)

The supercritical CO₂ used instead of water to stimulate low permeability formation. Supercritical CO₂ conditions are temperature of over 31.04°C and pressure of 7.38 MPa (Fig. 17). The CO₂ enhanced shale gas recovery method generally used after primary production. Refracturing the shale formation takes place for the injection of CO₂, N₂ and CO₂-N₂ to enhance the recovery of methane gas. The CO₂ storage mechanism includes hydrodynamic trapping, adsorption trapping, residual trapping, dissolution trapping and mineral trapping. Hydrodynamic trapping in which CO₂ remains as free fluid but gets trapped due to low permeability. Adsorption trapping in which CO₂ gets adsorbed to shale and desorb the methane molecules. Dissolution trapping is dissolving the CO₂ in formation water. Mineral trapping is the trapping of CO₂ to shale rock due to mineral precipitation. Residual trapping in which the moveable CO₂ phase transformed into the immobile phase.

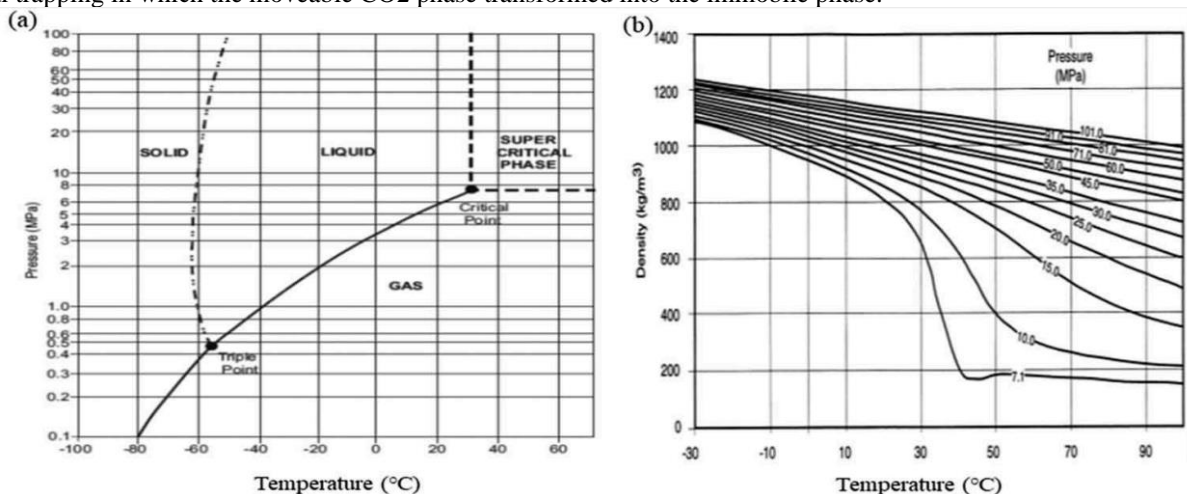


Fig. 17 (a) CO₂ phase and (b) CO₂ density at different temperatures (Liu, Li, Yang, & Agarwal, 2019)

The shale formations are fractured hydraulically to increase the permeability and supercritical CO₂ fracturing along with CO₂ adsorption for methane gas recovery from shale reservoirs (Fig. 18). The density of CO₂ will increase with increase in pressure and decrease in temperature. At low temperature, pressure has minimal effect on the change of density of CO₂ (Fig. 9). The shale rock influence by adsorbing gas CO₂ changing rock physically and chemically, which can result in increased recovery of methane gas.

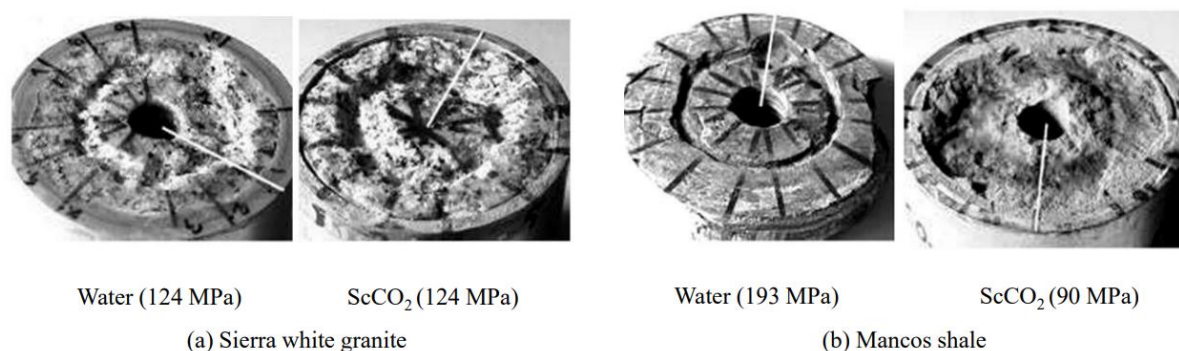


Fig.18 Core samples to understand fracturing influence under water and supercritical CO₂ respectively (Kolle, 2000; Li et al., 2018a)

These are core samples explaining exposure water and ScCO₂ on shale rock. Damage imposed by fracturing rock at different pressures shows ScCO₂ is more prominent to use for shale fracturing because of more penetration and destruction if compared with water. ScCO₂ at lower pressure range, maximum impact can be seen on rock samples compared with water and CO₂ pressure reduction almost by 50% and 15% respectively (Zhou et al., 2019).

REFERENCES

- [1] Goodman, A., Sanguinito, S., Kutchko, B., Natesakhawat, S., Cvetic, P., & Allen, A. J. (2020). Shale pore alteration: Potential implications for hydrocarbon extraction and CO₂ storage. *Fuel*, 265, 116930. doi:10.1016/j.fuel.2019.116930
- [2] Li, Z., & Elsworth, D. (2019). Controls of CO₂-N₂ gas flood ratios on enhanced shale gas recovery and ultimate CO₂ sequestration. *Journal of Petroleum Science and Engineering*, 179, 1037-1045. doi:10.1016/j.petrol.2019.04.098
- [3] Yin, H., Zhou, J., Jiang, Y., Xian, X., & Liu, Q. (2016). Physical and structural changes in shale associated with supercritical CO₂ exposure. *Fuel*, 184, 289-303. doi:10.1016/j.fuel.2016.07.028
- [4] Iddphonce, R., Wang, J., & Zhao, L. (2020). Review of CO₂ injection techniques for enhanced shale gas recovery: Prospect and challenges. *Journal of Natural Gas Science and Engineering*, 77, 103240. doi:10.1016/j.jngse.2020.103240
- [5] Huang, X., Xue, J., & Li, X. (2020). Adsorption Behavior of CH₄ and C₂H₆ on Shale under the Influence of CO₂ and Flue Gas. *Energy & Fuels*, 34(5), 5689-5695. doi:10.1021/acs.energyfuels.0c00339
- [6] Elliott, J. R., Suresh, S. J., & Donohue, M. D. (1990). A simple equation of state for non-spherical and associating molecules. *Industrial & Engineering Chemistry Research*, 29(7), 1476-1485. doi:10.1021/ie00103a057
- [7] Brunauer, S., Emmett, P. H., & Teller, E. (1938). Adsorption of Gases in Multimolecular Layers. *Journal of the American Chemical Society*, 60(2), 309-319. doi:10.1021/ja01269a023
- [8] U.S. Energy Information Administration (EIA). (2020). Retrieved 11 August 2020, from https://www.eia.gov/analysis/studies/worldshalegas
- [9] Liu, Y., Hou, J., & Wang, C. (2020). Absolute Adsorption of CH₄ on Shale with the Simplified Local-Density Theory. *SPE Journal*, 25(01), 212-225. doi:10.2118/199344-pa
- [10] Nesbitt, B. 2006. Handbook of Pumps and Pumping: Pumping Manual International, Elsevier
- [11] Zou, J., Rezaee, R., Xie, Q., You, L., Liu, K., & Saeedi, A. (2018). Investigation of moisture effect on methane adsorption capacity of shale samples. *Fuel*, 232, 323-332. doi: 10.1016/j.fuel.2018.05.167
- [12] Mahmoud, M., Hamza, A., Hussein, I., Eliebid, M., Kamal, M., & Abouelresh, M. et al. (2020). Carbon dioxide EGR and sequestration in mature and immature shale: Adsorption study. *Journal Of Petroleum Science And Engineering*, 188, 106923. doi: 10.1016/j.petrol.2020.106923
- [13] Liu, D., Agarwal, R., & Li, Y. (2017). Numerical simulation and optimization of CO₂ enhanced shale gas recovery using a genetic algorithm. *Journal of Cleaner Production*, 164, 1093-1104. doi:10.1016/j.jclepro.2017.07.040
- [14] Romero-Sarmiento, M., Pillot, D., Letort, G., Lamoureux-Var, V., Beaumont, V., Huc, A., & Garcia, B. (2015). New Rock-Eval Method for Characterization of Unconventional Shale Resource Systems. *Oil & Gas Science and Technology – Revue Des IFP Energies Nouvelles*, 71(3), 37. doi:10.2516/ogst/2015007
- [15] Luan, Xinyuan & Di, Bangrang & Wei, Jianxin & Zhao, Jian-Guo & Li, Xiangyang. (2016). Creation of synthetic samples for physical modelling of natural shale: Synthetic samples for physical modelling. *Geophysical Prospecting*. 64. 10.1111/1365-2478.12382.
- [16] Huo, P., Zhang, D., Yang, Z., Li, W., Zhang, J., & Jia, S. (2017). CO₂ geological sequestration: Displacement behavior of shale gas methane by carbon dioxide injection. *International Journal of Greenhouse Gas Control*, 66, 48-59. doi:10.1016/j.ijggc.2017.09.001
- [17] Guo, W., Hu, Z., Zhang, X., Yu, R., & Wang, L. (2017). Shale gas adsorption and desorption characteristics and its effects on shale permeability. *Energy Exploration & Exploitation*, 35(4), 463-481. doi:10.1177/0144598716684306
- [18] Li, Z., & Elsworth, D. (2019). Controls of CO₂-N₂ gas flood ratios on enhanced shale gas recovery and ultimate CO₂ sequestration. *Journal of Petroleum Science and Engineering*, 179, 1037-1045. doi:10.1016/j.petrol.2019.04.098
- [19] Chen, T., Feng, X., & Pan, Z. (2018). Experimental study on kinetic swelling of organic-rich shale in CO₂, CH₄ and N₂. *Journal of Natural Gas Science and Engineering*, 55, 406-417. doi:10.1016/j.jngse.2018.04.027
- [20] Bhuiyan, M. H., Agofack, N., Gawel, K. M., & Cerasi, P. R. (2020). Micro- and Macroscale Consequences of Interactions between CO₂ and Shale Rocks. *Energies*, 13(5), 1167. doi:10.3390/en13051167
- [21] Rani, S., Padmanabhan, E., & Prusty, B. K. (2019). Review of gas adsorption in shales for enhanced methane recovery and CO₂ storage. *Journal of Petroleum Science and Engineering*, 175, 634-643. doi:10.1016/j.petrol.2018.12.081
- [22] Liu, D., Li, Y., Yang, S., & Agarwal, R. K. (2019). CO₂ sequestration with enhanced shale gas recovery. *Energy Sources, Part A: Recovery, Utilization, and Environmental Effects*, 1-11. doi:10.1080/15567036.2019.1587069
- [23] Zhou, J., Jin, Z., & Luo, K. H. (2019). Effects of Moisture Contents on Shale Gas Recovery and CO₂ Sequestration. *Langmuir*, 35(26), 8716-8725. doi:10.1021/acs.langmuir.9b00862

- [24] Lu, Y., Ao, X., Tang, J., Jia, Y., Zhang, X., & Chen, Y. (2016). Swelling of shale in supercritical carbon dioxide. *Journal of Natural Gas Science and Engineering*, 30, 268-275. doi:10.1016/j.jngse.2016.02.011
- [25] Polanyi, M. (1963). The Potential Theory of Adsorption. *Science*, 141(3585), 1010-1013. doi:10.1126/science.141.3585.1010
- [26] Tesson, S., & Firoozabadi, A. (2019). Deformation and Swelling of Kerogen Matrix in Light Hydrocarbons and Carbon Dioxide. *The Journal of Physical Chemistry C*, 123(48), 29173-29183. doi:10.1021/acs.jpcc.9b04592
- [27] Zhao, Y., Wang, C., Zhang, Y., & Liu, Q. (2019). Experimental Study of Adsorption Effects on Shale Permeability. *Natural Resources Research*, 28(4), 1575-1586. doi:10.1007/s11053-019-09476-7
- [28] Pang, Y., Chen, S., Soliman, M. Y., Morse, S. M., & Hu, X. (2019). Evaluation of Matrix Swelling Behavior in Shale Induced by Methane Sorption under Triaxial Stress and Strain Conditions. *Energy & Fuels*, 33(6), 4986-5000. doi:10.1021/acs.energyfuels.9b00708
- [29] Wang, H., Qu, Z., Yin, Y., Bai, J., & Yu, B. (2018). Review of Molecular Simulation Method for Gas Adsorption/desorption and Diffusion in Shale Matrix. *Journal of Thermal Science*, 28(1), 1-16. doi:10.1007/s11630-018-1053-9
- [30] Lyu, Q., Long, X., Ranjith, P.G., et al. Experimental investigation on the mechanical properties of a low-clay shale with different adsorption times in sub-/supercritical CO₂. *Energy* 2018b, 147: 1288-1298
- [31] Yin, H., Zhou, J., Xian, X., et al. Experimental study of the effects of sub- and super-critical CO₂ saturation on the mechanical characteristics of organic-rich shales. *Energy* 2017, 132: 84-95.
- [32] Zhou, J., Hu, N., Xian, X., Zhou, L., Tang, J., Kang, Y., & Wang, H. (2019). Supercritical CO₂ fracking for enhanced shale gas recovery and CO₂ sequestration: Results, status and future challenges. *Advances in Geo-Energy Research*, 3(2), 207-224. doi:10.26804/ager.2019.02.10
- [33] Kolle, J.J. Coiled-tubing drilling with supercritical carbon dioxide. Paper SPE 65534 Presented at SPE/CIM International Conference on Horizontal Well Technology, Calgary, Alberta, Canada, 6-8 November, 2000
- [34] Coats, K., & Smith, B. (1964). Dead-End Pore Volume and Dispersion in Porous Media. *Society of Petroleum Engineers Journal*, 4(01), 73-84. doi:10.2118/647-pa
- [35] Middleton, R. S., Gupta, R., Hyman, J. D., & Viswanathan, H. S. (2017). The shale gas revolution: Barriers, sustainability, and emerging opportunities. *Applied Energy*, 199, 88-95. doi:10.1016/j.apenergy.2017.04.034
- [36] Kim, T. H., Cho, J., & Lee, K. S. (2017). Evaluation of CO₂ injection in shale gas reservoirs with multi-component transport and geomechanical effects. *Applied Energy*, 190, 1195-1206. doi:10.1016/j.apenergy.2017.01.047
- [37] Mohagheghian, E., Hassanzadeh, H., & Chen, Z. (2019). CO₂ sequestration coupled with enhanced gas recovery in shale gas reservoirs. *Journal of CO₂ Utilization*, 34, 646-655. doi:10.1016/j.jcou.2019.08.016
- [38] Huang, L., Ning, Z., Wang, Q., Ye, H., Chen, Z., Sun, Z., . . . Qin, H. (2018). Enhanced gas recovery by CO₂ sequestration in marine shale: A molecular view based on realistic kerogen model. *Arabian Journal of Geosciences*, 11(15). doi:10.1007/s12517-018-3762-5
- [39] Jia, B., Tsau, J., & Barati, R. (2018). Different Flow Behaviors of Low-Pressure and High-Pressure Carbon Dioxide in Shales. *SPE Journal*, 23(04), 1452-1468. doi:10.2118/191121-pa
- [40] Eshkalak, M. O., Al-Shalabi, E. W., Sanaei, A., Aybar, U., & Sepehrnoori, K. (2014). Simulation study on the CO₂-driven enhanced gas recovery with sequestration versus the re-fracturing treatment of horizontal wells in the U.S. unconventional shale reservoirs. *Journal of Natural Gas Science and Engineering*, 21, 1015-1024. doi:10.1016/j.jngse.2014.10.013
- [41] Shang, Z., Dong, L., Niu, L., & Shi, H. (2019). Adsorption of Methane, Nitrogen, and Carbon Dioxide in Atomic-Scale Fractal Nanopores by Monte Carlo Simulation I: Single-Component Adsorption. *Energy & Fuels*, 33(11), 10457-10475. doi:10.1021/acs.energyfuels.9b01405
- [42] Pang, Y., Tian, Y., Soliman, M. Y., & Shen, Y. (2019). Experimental measurement and analytical estimation of methane absorption in shale kerogen. *Fuel*, 240, 192-205. doi:10.1016/j.fuel.2018.11.144
- [43] Du, X., Gu, M., Liu, Z., Zhao, Y., Sun, F., & Wu, T. (2019). Enhanced Shale Gas Recovery by the Injections of CO₂, N₂, and CO₂/N₂ Mixture Gases. *Energy & Fuels*, 33(6), 5091-5101. doi:10.1021/acs.energyfuels.9b00822
- [44] Liu, J., Xie, H., Wang, Q., Chen, S., & Hu, Z. (2019). The Effect of Pore Size on Shale Gas Recovery with CO₂ Sequestration: Insight into Molecular Mechanisms. *Energy & Fuels*, 33(4), 2897-2907. doi:10.1021/acs.energyfuels.8b04166
- [45] Cao, J., Liang, Y., Masuda, Y., Koga, H., Tanaka, H., Tamura, K., . . . Matsuoka, T. (2019). Molecular Simulation of Methane Adsorption Behavior in Kerogen Nanopores for Shale Gas Resource Assessment. *International Petroleum Technology Conference*. doi:10.2523/19216-ms
- [46] Kutchko, B., Sanguinito, S., Natesakhawat, S., Cvetic, P., Culp, J. T., & Goodman, A. (2020). Quantifying pore scale and matrix interactions of SCCO₂ with the Marcellus shale. *Fuel*, 266, 116928. doi:10.1016/j.fuel.2019.116928
- [47] Goodman, A., Sanguinito, S., Kutchko, B., Natesakhawat, S., Cvetic, P., & Allen, A. J. (2020). Shale pore alteration: Potential implications for hydrocarbon extraction and CO₂ storage. *Fuel*, 265, 116930. doi:10.1016/j.fuel.2019.116930
- [48] Sui, H., Pei, P., Su, Q., Ding, W., & Mao, R. (2019). Study of Temperature Effects on Economic Performance of CO₂ Enhanced Shale Gas Recovery. *Journal of Energy Resources Technology*, 142(3). doi:10.1115/1.4044577
- [49] Sun, Y., Li, S., Sun, R., Liu, X., Pu, H., & Zhao, J. (2020). Study of CO₂ Enhancing Shale Gas Recovery Based on Competitive Adsorption Theory. *ACS Omega*. doi:10.1021/acsomega.0c03383
- [50] Huang, J., Jin, T., Barrufet, M., & Killough, J. (2020). Evaluation of CO₂ injection into shale gas reservoirs considering dispersed distribution of kerogen. *Applied Energy*, 260, 114285. doi:10.1016/j.apenergy.2019.114285